

ROTOR DROP TEST STAND FOR AMB ROTATING MACHINERY PART II : STEADY STATE ANALYSIS AND COMPARISON TO EXPERIMENTAL RESULTS

Krishnaswamy Ramesh

R. Gordon Kirk

Mechanical Engineering Dept., Virginia Tech, Blacksburg, VA, USA

ABSTRACT

A PC based finite element program is being developed for advanced concept rotor bearing systems, including those utilizing active magnetic bearings (AMB). The finite element program is aimed at modeling the rotor-bearing systems, to perform the stability analysis and unbalance response calculations. This paper presents the results of the stability analysis and unbalance response calculations of the AMB rotor drop test stand, which has been described in Part I of this paper. The paper also compares the analytical and the experimental results obtained, for the damped critical speeds and the unbalance response.

INTRODUCTION

The increase in high speed turbomachinery applications, has led to a significant progress in the study of rotor dynamics in the last decade. The evaluation of the dynamic stability and response to unbalance has become a standard calculation procedure for all new turbomachinery designs. The use of finite element in rotor dynamics dates back to the 1970's. The usual calculation procedure used in rotor dynamics has been described in several papers published in early to mid-seventies [1,2,3,5,6]. Ruhl and Booker [2] formulated a distributed parameter finite element model based on the Euler-Bernoulli beam. Since then the modeling has undergone a lot of modifications, enhancing the model to include the effects of rotary inertia, gyroscopic moments, shear deformation and axial load [4,7]. The current program models the rotor based on the Timoshenko beam theory as developed by Nelson [7].

The majority of the industry standard codes are based on the well established transfer matrix method, for the stability and unbalance response calculations. The transfer matrix stability programs are capable of only solving for a finite number of eigenvalues, usually the lowest eigenvalues. In the recent past, the finite element method has gained a lot of importance in the field of rotor dynamics. The use of finite element method for the formulation makes it possible to model increasingly complex problems, and recent

advances in digital computers have made the computations of large ordered problems feasible.

Another technology that has gained acceptance in recent years is the use of active magnetic bearings for industrial turbomachinery [8,9]. The advances in active magnetic bearing (AMB) technology present a new challenge to rotordynamicists. The rotor dynamic analysis of a machinery supported on AMB is complicated by the fact that the stiffness and damping properties of the magnetic bearing are a function of the whirl frequency rather than the running speed. Secondly, the position of the sensors, which feed back the displacement of the rotor to the bearings, are, in general, not aligned with the bearings. The non collocated positions of the sensors pose as additional problems, when the standard transfer matrix method is used for the analysis. However, recent work [10,11] has been done in modifying the transfer matrix solution procedure to cope with these two characteristics of AMB supported rotors. The finite element method has a distinct advantage in this regard. The sensor noncollocation can be conveniently handled and the usual iterative procedure of the transfer matrix method is not necessary, when the finite element method is used.

This paper compares the results of the damped eigenvalue analysis of the finite element program with the experimental results. The program accounts for sensor noncollocation and includes the evaluation of the eigenvalues based on the frequency dependent bearing properties. The validity of the finite element program was evaluated by comparing the results of the stability analysis to the well established transfer matrix codes, in previous work [12]. The paper also presents results of the unbalance response calculations of the AMB test rotor.

STABILITY ANALYSIS

The rotor shown in Fig. 1, was modeled using 39 elements. The rotor has a thin shell cross-section, typical of aircraft jet engine design. It is coupled to the gear-box through a

dry diaphragm type coupling. The rotor was modeled along with the coupling shaft and the gear-box pinion. The rotor weighs about 300 lb. and is about 230 mm in length. The pinion shaft is supported on two fluid bearings. The stiffness of the fluid film bearings were calculated and were relatively higher than the magnetic bearing stiffness. The operating speed of the AMB rotor is 8000 rpm.

The results generated by the finite element program for the stability analysis were compared to the damped eigenvalues obtained experimentally, by exciting the rotor using the magnetic bearings. The stiffness and damping of the magnetic bearings, as a function of frequency, were supplied by the magnetic bearing manufacturer. Initially, the undamped critical speeds were calculated. Damping was then included in the model, and the damped eigenvalues were evaluated. The comparison of the analytical and experimental eigenvalues are as shown in Table 1.

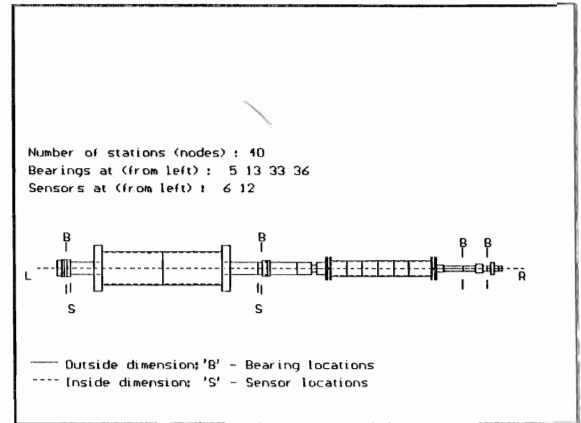


FIGURE 1 : Rotor model used for the analysis

Table 1. Comparison of results from the FE program and the experimental observations.

Mode	Finite Element Analysis				Obtained from test rig
	Collocated		Noncollocated		
	Undamped freq. (Hz)	Damped freq. (Hz)	Undamped freq. (Hz)	Damped freq. (Hz)	
1	48.36	47.42	48.61	47.70	46-50
2	57.61	55.12	56.50	53.85	(not observed)
3	112.20	110.78	112.28	110.86	102-107

From the results of the undamped and damped analysis, it can be seen that the frequencies drop as the damping is added to the system. This is in agreement with the theory. The influence of the sensor positions can also be seen from the results. The first and third frequencies increase, though by a small amount, as the sensors are moved inboard from the collocated positions. This is to be expected, because moving the sensors inboard, pulls the rotor down in the first and third modes, which essentially increase the stiffness for those modes. This results in an increase in the frequencies for the inboard sensor position. Similarly, for the second mode, the inboard sensor position decreases the stiffness and hence the frequency drops. The second mode was not observed in the excitation of the rotor, since both the magnetic bearings were excited in-phase.

UNBALANCE RESPONSE

The rotor has 4 location (planes) on which weights can be conveniently added. The four planes are the two disks (with 30 equally spaced holes drilled axially along a circle of diameter of 10 in.) and the hub of the coupling at the rotor end and the pinion end. Trial weights were added at these four locations, separately, and the rotor speed was increased to 5000 rpm. The rotor was then allowed to coast down on the magnetic bearings. Currently, there are 7 probes on the rotor for the measuring the displacement - the two sensors of the magnetic bearings (two at each of the magnetic bearing), one in the axial direction, and one probe each at the two ends of the coupling. The readings of the probes were recorded at every 50 rpm increment using the ADRE data acquisition system.

The test rig was balanced by a multiplane least squares method to achieve the lowest possible residual unbalance distribution. The trial weight runs were made with a weight of 4.66 gms. located in the rotor disk inboard and outboard planes, and at a radius of 127 mm. After the rotor was balanced, additional runs were made with the same trial weight in each of these planes. The data was captured and reduced for all channels. Figs. 2 to 5 show the response at the two magnetic bearing sensor locations for the unbalance weight at the inboard disk. Figs. 6 to 9 show the response at the two magnetic bearing sensor locations for the unbalance weight at the outboard disk. It must be pointed out that the magnetic bearing sensors have a sensitivity of 600 mV/mil, and since this cannot be set on the ADRE data acquisition system, the sensitivity was set at 304-309 for the above sensors. Hence, the amplitudes (peak-peak) shown in Figs. 2 to 9 are twice the actual amplitudes (peak-peak).

Figures 2 and 3 show the response of the magnetic bearing sensor, at the outboard location. The phase data shows a slow rolling phase with no clear indication of a critical speed. Figures 4 and 5 show the response of the sensors at the inboard location, where the unbalance weight was added. The amplitude shows an increasing trend with a maximum around 2500 rpm, but the curve is still too flat to specify the location of the critical speeds. The damping seems to be relatively high, and this prevents any sharp rise in amplitude.

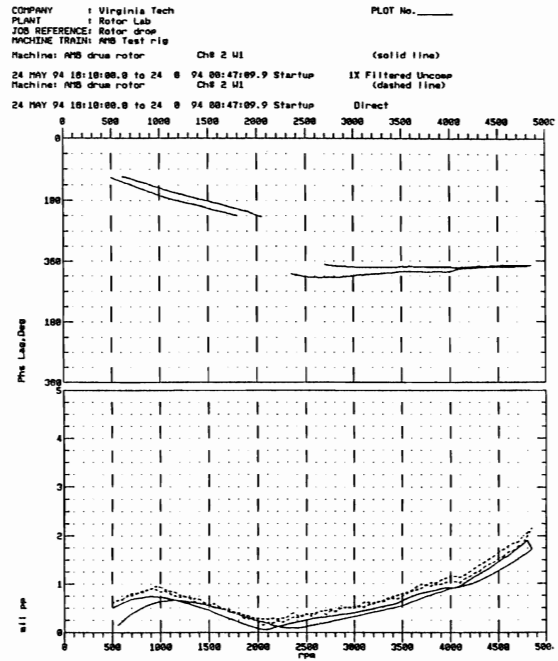


FIGURE 3 : Response at outboard location (probe #2) the unbalance at inboard location

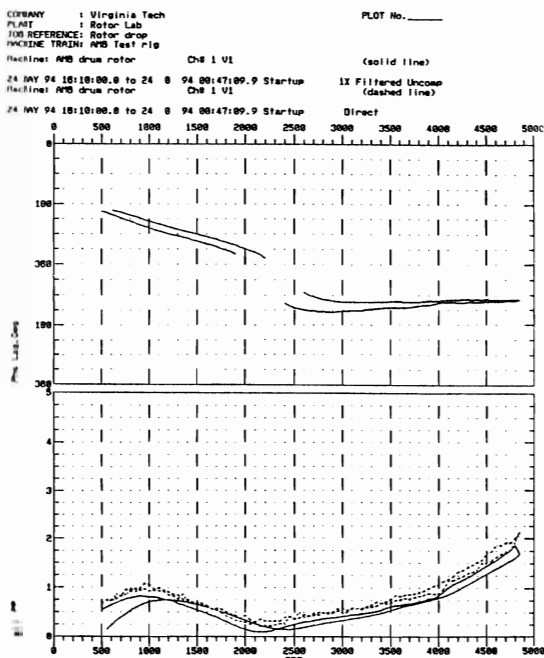


FIGURE 2 : Response at outboard location (probe #1) for the unbalance at inboard location

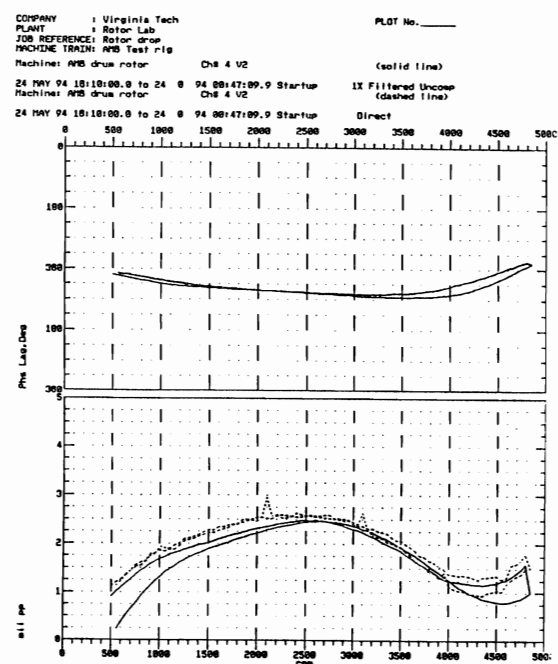


FIGURE 4 : Response at inboard location (probe #4) the unbalance at inboard location

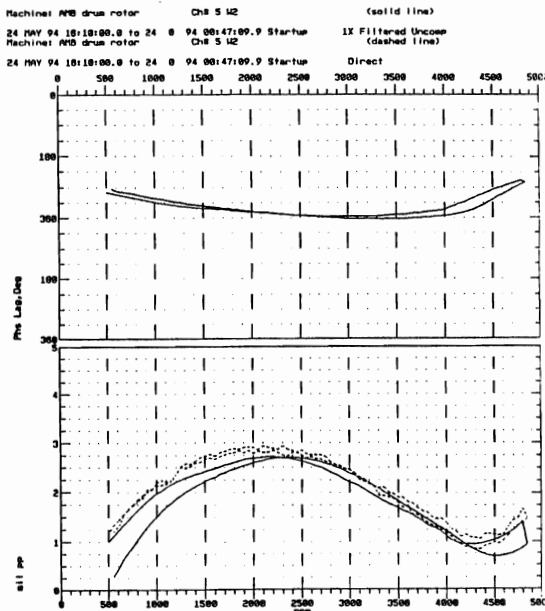


FIGURE 5 : Response at inboard location (probe #5) the unbalance at inboard location

and channel #5, that the amplitudes sensed by both the sensors in each of the planes, are of comparable amplitudes, indicating a circular response.

Figures 6 and 7 show the response of the sensors at the outboard location, where the unbalance weight was added. The amplitude seems to have an increasing trend, but again seems to indicate high damping. The curves in Figs. 8 and 9 show the response at the inboard location. The two solid lines on each of these plots correspond to run-up and run-down of the rotor. It can be seen that the two curves almost run together. It can also be noticed from the plots that the response increases at the locations of the unbalance. But the response at the opposite end does not show any significant information. This is due to the fact that the system has residual unbalance and this combined with the run-out, which keeps changing, distorts the low level amplitudes.

Figures 10 and 11 show the unbalance response of the rotor at the four sensor planes, as evaluated by the finite element program. The frequency dependent bearing parameters, supplied by the bearing manufacturer were used in the finite element program for the above analysis. Comparing the curves in Fig. 10 and Figs. 2 to 5, it can be seen that the amplitude ranges are quite agreeable. The curve for probe #4 (i.e., channel #4) from Fig. 10 shows the same trend as the curve in Fig. 4. The absence of a distinct critical speed in the Figs. 10 and 11 are in complete agreement with the data obtained from the experiment. Also the curves that correspond to the response at the unbalance locations, agree quite closely. It can be noted the from the curves for channel #1 and channel #2, and similarly for channel #4

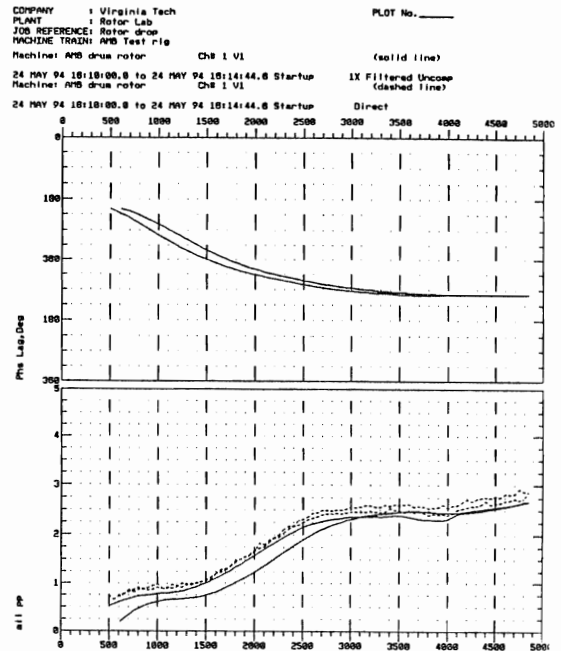


FIGURE 6 : Response at outboard location (probe #1) the unbalance at outboard location

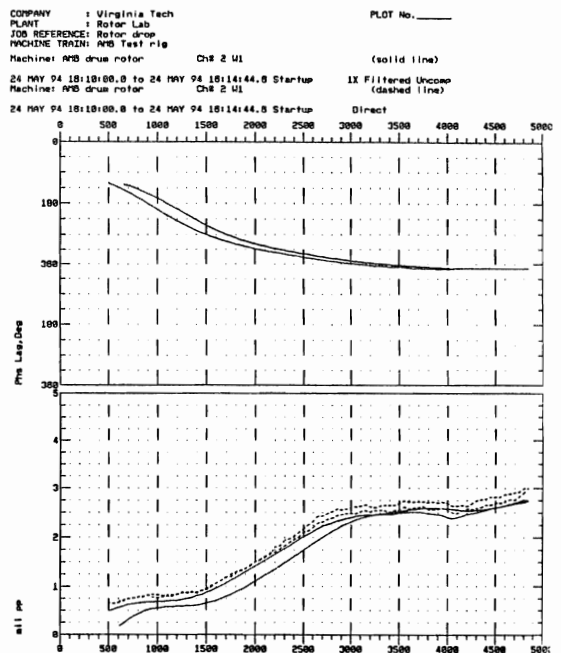


FIGURE 7 : Response at outboard location (probe #2) the unbalance at outboard location

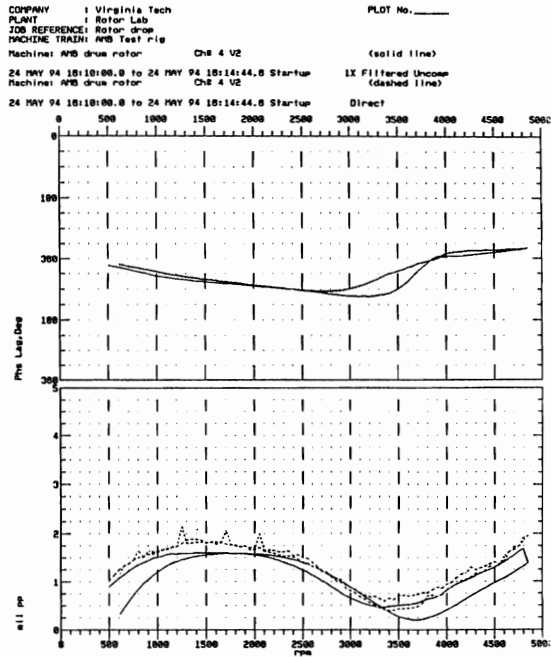


FIGURE 8 : Response at inboard location (probe #4) the unbalance at outboard location

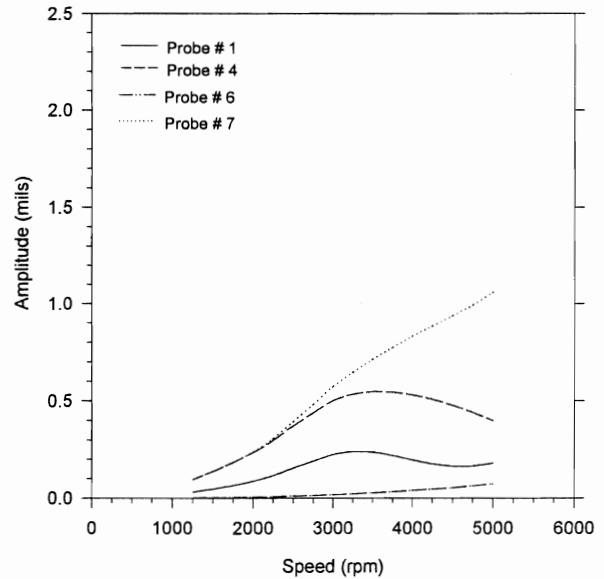


FIGURE 10 : Response at the probe locations as calculated by the finite element program for unbalance at inboard location

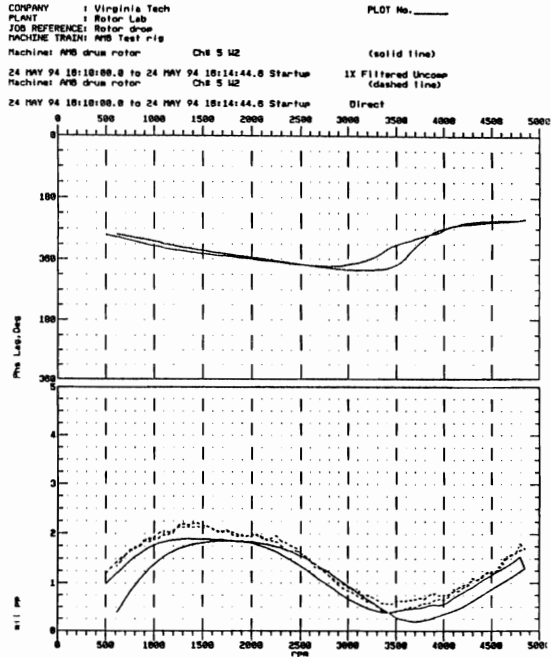


FIGURE 9 : Response at inboard location (probe #5) the unbalance at outboard location

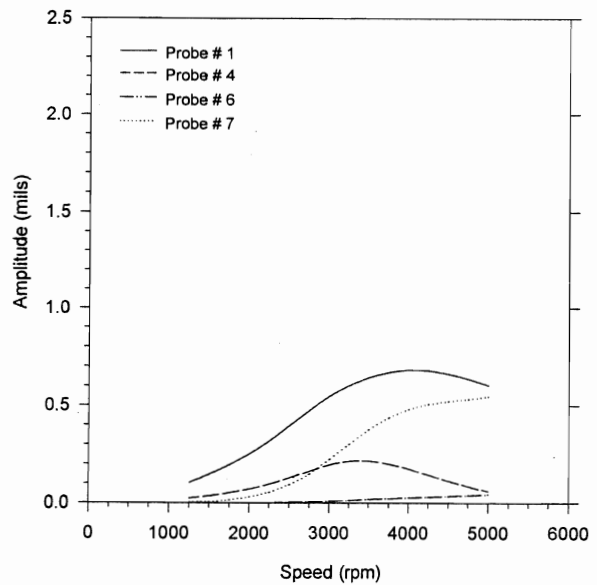


FIGURE 11 : Response at the probe locations as calculated by the finite element program for unbalance at outboard location

CONCLUSIONS

1. The comparison of the results of the stability analysis, as shown in Table 1, show that the sensor location must be considered in evaluation of the critical speeds. Also the critical speeds, observed by the excitation of the rotor, change as predicted by the finite element program for the inboard sensor positions.

2. The results of the critical speed analysis as calculated by the finite element program are in close agreement with the critical speeds obtained by exciting the rotor.

3. The response levels as calculated by the finite element program agree closely with those obtained from the experiment, at the plane of the unbalance location.

4. The response amplitudes at the opposite end from the applied unbalance location do not match exactly due to the residual unbalance and the changing run-out during each run of the rotor.

ACKNOWLEDGMENTS

This research was sponsored by the Virginia Center for Innovative Technology with additional grants from Magnetic Bearing Inc., Dresser-Rand Turbo Division and Pratt & Whitney Aircraft.

REFERENCES

1. Ruhl, R.L., "Dynamics of Distributed Parameter Rotor Systems : Transfer Matrix and Finite Element Techniques," PhD dissertation, Cornell University, Ithaca, NY, 1970.
2. Ruhl, R.L., and Booker, J.F., "A Finite Element Model for Distributed Parameter Turbomotor Systems," ASME Journal of Engineering for Industry, pp. 128-132, 1972.
3. Lund, J.W., "Stability and Damped Critical Speeds of a Flexible Rotor in Fluid-film Bearings," ASME Journal of Engineering for Industry, Series B, 96(2), pp. 509-517, 1974.
4. Nelson, H.D., and McVaugh, J.M., "The Dynamics of Rotor-Bearing Systems using Finite Elements," ASME Journal of Engineering for Industry, 98(2), pp. 593-600, 1975.
5. Bansal, P.N., and Kirk, R.G., "Stability and Damped Critical Speeds of Rotor-Bearing Systems," ASME Journal of Engineering for Industry, 97(B4), pp. 1325-1332, 1975.

6. Kirk, R.G., "Stability and Damped Critical Speeds : How to Calculate and Interpret the Results," CAGI Technical DIGEST, 12(2), pp. 375-383, 1980.

7. Nelson, H.D., "A Finite Rotating Shaft Element Using Timoshenko Beam Theory," Journal of Mechanical Design, 102(10), pp. 793-803, 1980.

8. Hustak, J., Kirk, R.G., and Schoeneck, K.A., "Analysis and Test Results of Turbocompressors Using Active Magnetic Bearings," Lubrication Engineering, 43(5), pp. 356-362, 1987.

9. Kasarda, M., Alaire, P.E., Humphries, R.R., and Barrett, L.E., "A Magnetic Damper for First Mode Vibration Reduction in Multimass Flexible Rotors," Gas Turbine and Aeroengine Congress and Exposition, Toronto, ASME Paper 89-GT-213, 1989.

10. Kirk, R.G., Keesee, J., Ohanehi, D., and Pinckney, P., "Influence of Active Magnetic Bearing Sensor Location on the Critical Speeds of Turbomachinery," presented at ASME Design Technical Conference, Montreal, Quebec, Canada, Rotating Machinery Dynamics, ASME DE-Vol. 18-1, pp. 309-316, 1989.

11. Rawal, D., Keesee, J., and Kirk, R.G., "The Effect of Sensor Location on the Forced Response Characteristics of Rotors with Active Magnetic Bearings," ASME Conference Proceedings, DE-Vol. 35, pp. 209-218, 1991.

12. Ramesh, K., and Kirk, R.G., "Subharmonic Resonance Stability Prediction for Turbomachinery with Active Magnetic Bearings," Proceedings of the Third International Symposium on Magnetic Bearings, pp. 113-122, 1992.